SCIENCE CHINA
Information Sciences

• RESEARCH PAPER •

November 2024, Vol. 67, Iss. 11, 212206:1–212206:14
https://doi.org/10.1007/s11432-023-4018-5

Finite-time PID control for nonlinear nonaffine systems

Zhiqing LIU[1], Ronghu CHI[2*], Biao HUANG[3] & Zhongsheng HOU[4]

[1]*College of Mathematics and Physics, Qingdao University of Science and Technology, Qingdao* 266061*, China;*
[2]*College of Automation and Electronic Engineering, Qingdao University of Science and Technology, Qingdao* 266061*, China;*
[3]*Department of Chemical and Materials Engineering, University of Alberta, Edmonton* AB T6G 2G6*, Canada;*
[4]*School of Automation, Qingdao University, Qingdao* 266071*, China*

Received 26 September 2023/Revised 9 January 2024/Accepted 23 February 2024/Published online 18 October 2024

Abstract This article proposes a finite-time proportional-integral-derivative (FT-PID) control method to fast stabilize the control system to achieve the desired performance within the predesignated time instants. For a considered nonaffined nonlinear system, we develop a new dynamic linearization approach to reformulate the system model as a linear data model (LDM) whose arguments are consistent with that used in the PID control law. Then, a projection algorithm is presented to estimate the unknown pseudo gradient vector of the LDM. Subsequently, an adaptive tuning algorithm is designed to update the three PID parameters by solving linear matrix inequalities in terms of the predesignated error precision and the finite-time instant. The finite-time convergence of the proposed FT-PID control system is shown mathematically, which guarantees a pre-specified error precision to be achieved within the predesignated finite-time instants. As a result, not only can the proposed FT-PID control save the control cost but it also improves the production efficiency. The simulation study verifies the results.

Keywords PID control, finite-time control, nonlinear nonaffine systems, linear data model, finite-time convergence

1 Introduction

Proportional-integral-derivative (PID) control has been the well-known controller in industrial processes [1–5] since it appeared in 1922 owing to its advantages of simplicity, robustness, and ease of implementation. It has been pointed out in [6] that 95 percent of industrial controllers are PID. From both theory and application points of view, however, there are still many challenging problems in improving the PID controllers to meet the requirements of the increasingly complex industrial processes [6–8].

First, how to select the proper controller parameters is one of the most critical issues to ensure PID control performance. Nowadays, many PID tuning methods have been developed through extensive practical applications, including the empirical method [9], Ziegler-Nichols method [10], the relay tuning method [11], Cohen-Coon method [12], virtual reference feedback tuning (VRFT) [13], and iterative feedback tuning (IFT) [14]. On the one hand, however, these methods [9–14] depend on either the closed-loop tests or the prior model information. On the other hand, these tuning methods [9–14] do not update the parameters adaptively in real time but keep them unchanged once the parameters have been obtained. These tuning methods may perform poorly if large uncertainties appear or the system changes. Therefore, a more critical issue than the first one is how to tune the PID parameters in real time to adapt to the system uncertainties and exogenous disturbances to enhance the PID robustness.

Recently, many adaptive PID tuning methods have been proposed [15,16], such as the fuzzy PID [17], neural network PID [18], and genetic PID [19]. It is noteworthy that the fuzzy PID depends on the fuzzy rule model obtained by the experience and the knowledge of the experts. On the other hand, neural network-based PID control might be too complex to implement in industrial control infrastructure and

* Corresponding author (email: ronghu_chi@qust.edu.cn)

has the inherent shortcomings of slow convergence and many uncertain parameters. The genetic PID control has a poor ability of optimization search and a limitation of premature convergence. Further, the selections of the proper membership functions, neural network structures, and fitness functions also depend on the available model knowledge of processes. To summarize, therefore, most of the existing adaptive PID tuning methods are model-dependent with computational complexity and poor convergence, which is the second challenge of the existing model-based PID tuning methods.

The third challenge of the existing PID control is how to break through their asymptotic stability problem in the sense of the corresponding infinite operation time to achieve a fast convergence with a shorter time. The reason lies in that, in many practical situations, the engineers expect to achieve a required control precision by a limited operation time interval for the purpose of minimizing the cost and improving the manufacturing efficiency. For example, in the control of unmanned vehicles [20], spacecraft attitude [21], and robotic manipulator [22], the tracking error is desired to converge to a specified bound with the designated time.

In [23–25], the finite-time stability (FTS) is proposed to guarantee that the system states do not go beyond a certain bound within a designated time interval for a given bounded initial condition. The early research has studied the FTS by using the open-loop control method, but that method lacks the ability of anti-disturbance. For this reason, the finite-time control (FTC) based on the system feedback attracts much attention [26–28]. A sufficient condition of FTS is proposed in [27] for linear time-invariant discrete systems. This result is further extended to linear time-varying discrete systems [29] by showing the necessary and sufficient conditions for FTS. Since then, several FTC methods have been proposed for linear discrete-time systems subject to input-output constraint [30] and time-delay [31, 32].

It is noteworthy that the practical plants are inherently nonlinear [33, 34]. Therefore, the FTC methods [26–32] that mainly focus on the linear systems may encounter many difficulties when applied to practice. Recently, Haddad and Lee [35] have discussed the FTS of nonlinear discrete-time autonomous dynamical systems via the Lyapunov function. Further, an FTS-based feedback control law [36] is presented for a discrete-time nonlinear dynamic system by minimizing a nonlinear nonquadratic performance function. The results of FTS have also been extended to nonlinear discrete-time stochastic systems [37]. Meanwhile, the FTS of nonlinearly parameterized systems [38, 39] and the neural network FTC [40, 41] have been studied, for example, the novel results on the fuzzy adaptive fixed-time quantized feedback control [42] and the adaptive finite-time tracking control [43] of nonlinear systems.

To summarize, although these results [35–41] are presented for nonlinear systems, some model information is still required, such as the parametric or affine structure information of the system. Further, a proper selection of the neural network [40, 41] also depends on some prior knowledge of the system. However, the real processes are increasingly complicated with large scales, high orders, strong uncertainties, and time-varying structures, such that their exact mathematical models are difficult to establish.

Data-driven control methods, including PID control [6–8], VRFT [13], IFT [14], and model free adaptive control (MFAC) [44, 45], have attracted much attention owing to their advantage of bypassing the modeling. PID control is data-driven inherently and has become popular in real industrial applications as discussed above. However, no result has been reported for its FTS design and analysis up to date.

Motivated by the above discussion, a new data-driven finite-time PID (FT-PID) control is proposed in this article by considering the challenges in the existing PID and the FTC design methods, where to endow the PID control and FTC methods with the data-driven property in both design and analysis, a strongly nonaffined nonlinear system is considered in this work without requiring any model information.

First, a novel dynamic linearization is presented following [44, 45] where the arguments are newly designed to make them consistent with the information used in the PID control law. The corresponding linear data model (LDM) obtained by virtue of the novel dynamic linearization is then updated in real time by developing an adaptive estimation algorithm for its unknown pseudo gradient parameters.

Second, to make the PID controller more adaptive and robust to the system uncertainties, an incremental PID controller is designed with the three PID parameters being time-varying. Then, a real-time tuning algorithm of the three PID parameters is developed by solving the linear matrix inequalities (LMIs). The estimation of the pseudo gradients together with their upper bounds is also included in the LMIs as the critical factors to address the nonlinear uncertainty of the system in real time.

Third, to make the PID control finite-time stable, the designed LMIs also include the error precision and the finite-time specifications, both of which are designated in advance to meet the practical requirement. Then, the stability of the FT-PID control is shown by defining a Lyapunov function and utilizing the Young's inequality. Both the theoretical analysis and the simulation results demonstrate that the proposed FT-PID control is capable of achieving a specified error precision within the predesignated finite-time instant, thus reducing the control cost and improving the production efficiency.

Compared with the existing PID methods [9–14], not only can the FTS of the proposed FT-PID be guaranteed, but also the PID parameters can be computed in real time. It does not require closed-loop tests beforehand or the model information of the system. Further, the theoretical analysis of the proposed FT-PID, especially under a data-driven framework for a nonaffined nonlinear system, is of most significance since few stability results of PID control have been reported up to date, even for linear systems under the model-based framework.

Compared with the existing FTC methods [26–32, 35–37], the proposed FT-PID control is data-driven without relying on the exact model information, which enhances its applicability in practice for complex nonlinear systems. Further, the proposed FT-PID contains an adaptive updating law of the pseudo gradient parameters of the LDM, thus improving its robustness against nonlinear uncertainties.

This paper consists of six sections. Section 2 gives preliminaries and problem statements. The FT-PID method is proposed in Section 3 and the convergence analysis is given in Section 4. Section 5 is the simulation study. Section 6 concludes the paper.

In this paper, T represents the transpose of a matrix; $\mathrm{diag}(a_1, a_2, \ldots, a_n)$ is a diagonal matrix consisting of $a_1, a_2, \ldots, a_n$. $|a|$ denotes the absolute value of a. The weighted norm of the vector $\boldsymbol{x}$ is defined as $\|\boldsymbol{x}\|_{\boldsymbol{Q}} := \sqrt{\boldsymbol{x}^{\mathrm{T}}\boldsymbol{Q}\boldsymbol{x}}$, where $\boldsymbol{Q}$ is a positive definite matrix. The matrix norm induced by $\|\boldsymbol{x}\|_{\boldsymbol{Q}}$ is denoted as $\|\boldsymbol{A}\|_{\boldsymbol{Q}} := \max_{\boldsymbol{x}\neq 0}\{\frac{\|\boldsymbol{A}\boldsymbol{x}\|_{\boldsymbol{Q}}}{\|\boldsymbol{x}\|_{\boldsymbol{Q}}}\}$. The symmetric terms in a matrix are represented by $*$.

Besides, Δ denotes the first-order difference operator, i.e., $\Delta x(k) = x(k) - x(k-1)$, and $\Delta^2 x(k) = \Delta x(k) - \Delta x(k-1)$.

As an important mathematical tool in this work, Young's inequality is presented as follows.

Young's inequality ([46])**.** Letting $p, q > 1$ and $\frac{1}{p} + \frac{1}{q} = 1$, then $\forall a, b > 0$ and $\forall \rho > 0$, we have

$$ab \leqslant \frac{\rho}{p}a^p + \frac{1}{q}\rho^{-\frac{q}{p}}b^q.$$

Particularly, if $p = q = 2$, one has

$$ab \leqslant \frac{\rho}{2}a^2 + \frac{1}{2\rho}b^2.$$

2 Problem formulation and finite-time convergence

2.1 Problem formulation

Consider a discrete-time nonaffined nonlinear system,

$$y(k+1) = f\left(y(k),\ y(k-1), \ldots, y(k-n_y), u(k),\ u(k-1), \ldots, u(k-n_u)\right), \tag{1}$$

where $k \in \mathbb{N}$ represents the time instant; $u(k) \in \mathbb{R}$ and $y(k) \in \mathbb{R}$ are the system input and output, respectively; $u(k) = 0$ and $y(k) = 0$ for $k < 0$; f is a nonlinear function; n_y and n_u are two positive constants denoting system orders.

Assumption 1 ([45])**.** The partial derivatives of $f(\cdot)$ with respect to its arguments are continuous.

Assumption 2 ([45])**.** The nonlinear system (1) is generalized Lipschitz continuous, that is,

$$|y(k_1+1) - y(k_2+1)| \leqslant b_L \left\|\boldsymbol{h}(k_1) - \boldsymbol{h}(k_2)\right\|,$$

for $\boldsymbol{h}(k_1) \neq \boldsymbol{h}(k_2)$ and $\forall k_1 \neq k_2,\ k_1, k_2 \geqslant 0$, where $\boldsymbol{h}(k_i) = [y(k_i)\ y(k_i-1)\ u(k_i)]^{\mathrm{T}}$ denotes the input-output vector, $i = 1, 2$, and $b_L > 0$ is a constant.

By nature, Assumption 2 is a special case of the assumption used in [45]. Further, only the existence of b_L is required in this work rather than its exact value. Comparatively, the main difference is that the vector $\boldsymbol{h}(\cdot)$ only contains the feedback information and control input that is used in the subsequent PID controller. According to [45], it is reasonable and satisfied by many practical systems, e.g., the robotic in motion [47] and the hydraulic system [48].

2.2 Definition of finite-time convergence

Similar to [29], a new definition of finite-time convergence is presented as follows.

Definition 1. Let $e(k) := y_d(k) - y(k)$ denote the tracking error, in which $y_d(k)$ is the desired output. Assume that the predesignated finite time instant is K and the specified error bound is c which is a small positive constant. For a constant $r > 0$ and a function $\beta(k) > 0$, if the conditions

(i) $$r\left(|e(0)|^2 + |\Delta e(0)|^2 + |\Delta^2 e(0)|^2\right) \leqslant c, \tag{2}$$

(ii) $$\beta(K)|e(K)|^2 < c \tag{3}$$

are satisfied, then we say that $e(k)$ is finite-time convergent. Further, let $\beta(k) := \theta^{K-k}$, $k \in \{1, 2, \ldots, K\}$ with $0 < \theta < 1$, then the condition (ii) implies that

$$|e(K)|^2 < c. \tag{4}$$

Since $e(k) = 0$ for $k < 0$, the condition (i) indeed means that the initial tracking error is bounded, which is commonly satisfied in practical control systems.

3 Finite-time PID controller design

Our objective is to develop a finite-time PID controller to make the tracking error converge to the desired error bound c within a predesignated finite time K, that is, $|e(K)|^2 < c$.

Note that the controlled system (1) is 'nonaffined nonlinear', which means that it is not only nonlinear but also nonaffined to the control input such that it is difficult or even impossible to design a controller since the control input is always coupled with the system state or output. To deal with this problem, a dynamic linearization data model is established as shown below to facilitate the subsequent design and analysis.

Lemma 1. For nonlinear system (1) satisfying Assumptions 1 and 2, one can find a time-varying vector $\boldsymbol{\phi}(k) \in \mathbb{R}^3$ to reformulate system (1) as an LDM,

$$\Delta y(k+1) = \boldsymbol{\phi}^{\mathrm{T}}(k)\Delta \boldsymbol{h}(k), \tag{5}$$

where $\Delta \boldsymbol{h}(k) = [\Delta y(k)\ \Delta y(k-1)\ \Delta u(k)]^{\mathrm{T}}$, $\boldsymbol{\phi}(k) = [\phi_1(k)\ \phi_2(k)\ \phi_3(k)]^{\mathrm{T}}$ denotes the pseudo gradient vector of system (1) with respect to its arguments, and $\|\boldsymbol{\phi}(k)\| \leqslant b_L$, which is defined in Assumption 2.

See Appendix A for the proof of Lemma 1.

Remark 1. Note that the LDM (5) is the same as the data model in [44] obtained by using a full form dynamic linearization method such that the system output can be described exactly by using both input and output over a moving time-window. However, it is also noted that the input and output (I/O) information presented in the newly established LDM (5) is the same as that used in the standard incremental PID controller such that the LDM is simplified by merely using I/O data over a shorter time-window. Therefore, the subsequent controller design, analysis, and computation are simplified.

Note that $\boldsymbol{\phi}(k)$ is unknown in (5), therefore, a projection algorithm is developed for its estimation,

$$\widehat{\boldsymbol{\phi}}(k) = \widehat{\boldsymbol{\phi}}(k-1) + \frac{\eta \Delta \boldsymbol{h}(k-1)[\Delta y(k) - \widehat{\boldsymbol{\phi}}^{\mathrm{T}}(k-1)\Delta \boldsymbol{h}(k-1)]}{\mu + \|\Delta \boldsymbol{h}(k-1)\|^2}, \tag{6}$$

where $\widehat{\boldsymbol{\phi}}(k) = [\widehat{\phi}_1(k)\ \widehat{\phi}_2(k)\ \widehat{\phi}_3(k)]^{\mathrm{T}}$ is the estimation of $\boldsymbol{\phi}(k)$; $\mu > 0$ and $\eta \in (0, 2)$ are some proper constants.

An FT-PID control method is designed,

$$u(k) = u(k-1) + \Gamma_P(k)\Delta e(k) + \Gamma_I(k)e(k) + \Gamma_D(k)\Delta^2 e(k), \tag{7}$$

$$\boldsymbol{\Gamma}(k) = \boldsymbol{L}(k)\boldsymbol{Q}^{-1}(k), \tag{8}$$

$$\begin{cases} \begin{bmatrix} -\boldsymbol{Q}(k) & * & * \\ \widehat{\boldsymbol{\Phi}}_{1,2}(k)\boldsymbol{Q}(k) - \widehat{\boldsymbol{\Phi}}_3(k)\boldsymbol{L}(k) & -\frac{\rho}{1+\rho}\boldsymbol{Q}(k+1) & * \\ \boldsymbol{C}_1\boldsymbol{Q}(k) + \boldsymbol{C}_2\boldsymbol{L}(k) & 0 & -\frac{1}{(1+\rho)\lambda^2}\boldsymbol{Q}(k+1) \end{bmatrix} < 0, & \text{(9a)} \\ \boldsymbol{Q}(k) > 0,\ \boldsymbol{Q}(k+1) > 0, & \text{(9b)} \\ \boldsymbol{Q}(0) > \boldsymbol{R}^{-1}, & \text{(9c)} \\ q_I(k+1) < \beta^{-1}(k+1), & \text{(9d)} \end{cases}$$

where $\lambda > 0$ and $\rho > 0$ are proper constants, and

$$\boldsymbol{\Gamma}(k) = \begin{bmatrix} \Gamma_P(k)\ \Gamma_I(k)\ \Gamma_D(k) \end{bmatrix},\ \boldsymbol{L}(k) = \begin{bmatrix} l_P(k)\ l_I(k)\ l_D(k) \end{bmatrix}, \boldsymbol{Q}(k) = \mathrm{diag}(q_P(k),\ q_I(k),\ q_D(k)),$$

$$\widehat{\boldsymbol{\Phi}}_{1,2}(k) = \begin{bmatrix} \widehat{\phi}_1(k) + \widehat{\phi}_2(k) & 0 & -\widehat{\phi}_2(k) \\ \widehat{\phi}_1(k) + \widehat{\phi}_2(k) & 1 & -\widehat{\phi}_2(k) \\ \widehat{\phi}_1(k) + \widehat{\phi}_2(k) - 1 & 0 & -\widehat{\phi}_2(k) \end{bmatrix},\ \widehat{\boldsymbol{\Phi}}_3(k) = \begin{bmatrix} \widehat{\phi}_3(k)\ \widehat{\phi}_3(k)\ \widehat{\phi}_3(k) \end{bmatrix}^{\mathrm{T}},$$

$$\boldsymbol{C}_1 = \begin{bmatrix} 1 & 0 & 0 \\ 0 & 0 & 1 \\ 0 & 0 & 0 \end{bmatrix},\ \boldsymbol{C}_2 = \begin{bmatrix} 0\ 0\ 1 \end{bmatrix}^{\mathrm{T}},\ \boldsymbol{R} = \mathrm{diag}(r,\ r,\ r).$$

In sum, the proposed FT-PID control approach consists of (6)–(9) where Eq. (6) is used to update the nonlinear uncertainty of the controlled system (1), and Eq. (8) is used to update the controller parameters $\Gamma_P(k)$, $\Gamma_I(k)$, $\Gamma_D(k)$ in real time by virtue of the feasible solutions of the LMI conditions (9), to achieve the finite-time convergence of the tracking error.

Remark 2. Different from the traditional PID control, the proposed FT-PID controller parameters $\Gamma_P(k)$, $\Gamma_I(k)$, $\Gamma_D(k)$ are time-varying and can be tuned by (8) and (9) in real time. As a result, the proposed FT-PID not only can adapt to the system uncertainties more effectively but also can drive the tracking error to the specified bound within the predesignated time interval once the other parameters are selected to satisfy the LMI conditions (9).

Remark 3. From (6)–(9), it is seen that no model information is needed in the proposed FT-PID control design. Further, the controller parameters are updated by (8) and (9) only utilizing the I/O data, which is different from the traditional tuning methods, such as Ziegler-Nichols method [10], the relay tuning method [11], and Cohen-Coon method [12], where either the closed-loop experiment or some model information is required. Therefore, the proposed FT-PID control (6)–(9) is a completely data-driven method, which facilitates its applications in complex practical processes.

Remark 4. The parameter r is of importance since it establishes the connection between the initial tracking error $e(0)$ and the error bound c, and is used to obtain the PID parameters $\Gamma_P(k)$, $\Gamma_I(k)$, $\Gamma_D(k)$. Therefore, the finite-time convergence relies on the initial tracking error. Specifically, the parameter $\boldsymbol{R} = \mathrm{diag}(r, r, r)$ in (9c) depends on the initial tracking error $e(0)$ and the specified error bound c according to the condition (i) in Definition 1, which implies that Eq. (9c) is a condition related to the designated c. On the other hand, the effect of K is reflected in $\beta(k)$ set in Definition 1, which is used in LMI condition (9d).

4 Convergence analysis

The convergence property of the FT-PID control (6)–(9) is summarized as follows.

Theorem 1. For nonlinear discrete-time system (1) under Assumptions 1 and 2 with $y_d(k) = y^* =$ const., the FT-PID control (6)–(9) with proper parameters can guarantee the following properties:

(i) The parameter estimation, $\widehat{\boldsymbol{\phi}}(k)$, is bounded $\forall k \in \mathbb{N}_+$;

(ii) The tracking error is finite-time convergent by the designated error bound c within time instant K, i.e., $|e(K)|^2 < c$.

Proof. (i) The boundedness of $\widehat{\boldsymbol{\phi}}(k)$. Letting $\widetilde{\boldsymbol{\phi}}(k) = \boldsymbol{\phi}(k) - \widehat{\boldsymbol{\phi}}(k) = [\widetilde{\phi}_1(k)\ \widetilde{\phi}_2(k)\ \widetilde{\phi}_3(k)]^{\mathrm{T}}$, it follows from (6) that

$$\widetilde{\boldsymbol{\phi}}(k) = \widetilde{\boldsymbol{\phi}}(k-1) - \frac{\eta\Delta\boldsymbol{h}(k-1)\widetilde{\boldsymbol{\phi}}^{\mathrm{T}}(k-1)\Delta\boldsymbol{h}(k-1)}{\mu + \|\Delta\boldsymbol{h}(k-1)\|^2} + \boldsymbol{\phi}(k+1) - \boldsymbol{\phi}(k). \tag{10}$$

Taking the norm of (10), one has

$$\|\widetilde{\boldsymbol{\phi}}(k)\| \leqslant \left\|\widetilde{\boldsymbol{\phi}}(k-1) - \frac{\eta\Delta\boldsymbol{h}(k-1)\widetilde{\boldsymbol{\phi}}^{\mathrm{T}}(k-1)\Delta\boldsymbol{h}(k-1)}{\mu + \|\Delta\boldsymbol{h}(k-1)\|^2}\right\| + 2b_L. \tag{11}$$

Since $\mu > 0$ and $0 < \eta < 2$, one can get

$$-2 + \frac{\eta\|\Delta\boldsymbol{h}(k-1)\|^2}{\mu + \|\Delta\boldsymbol{h}(k-1)\|^2} < 0,$$

and then,

$$\begin{aligned}
&\left\|\widetilde{\boldsymbol{\phi}}(k-1) - \frac{\eta\Delta\boldsymbol{h}(k-1)\widetilde{\boldsymbol{\phi}}^{\mathrm{T}}(k-1)\Delta\boldsymbol{h}(k-1)}{\mu + \|\Delta\boldsymbol{h}(k-1)\|^2}\right\|^2 \\
&= \left\|\widetilde{\boldsymbol{\phi}}(k-1)\right\|^2 + \left(-2 + \frac{\eta\|\Delta\boldsymbol{h}(k-1)\|^2}{\mu + \|\Delta\boldsymbol{h}(k-1)\|^2}\right)\frac{\eta[\widetilde{\boldsymbol{\phi}}^{\mathrm{T}}(k-1)\Delta\boldsymbol{h}(k-1)]^2}{\mu + \|\Delta\boldsymbol{h}(k-1)\|^2} < \left\|\widetilde{\boldsymbol{\phi}}(k-1)\right\|^2,
\end{aligned}$$

which together with (11) implies

$$\|\widetilde{\boldsymbol{\phi}}(k)\| \leqslant d\|\widetilde{\boldsymbol{\phi}}(k-1)\| + 2b_L \leqslant \cdots \leqslant d^k\|\widetilde{\boldsymbol{\phi}}(0)\| + \frac{2b_L(1-d^k)}{1-d}, \tag{12}$$

where $0 < d < 1$ is a constant.

Therefore, from (12), one can conclude that $\widetilde{\boldsymbol{\phi}}(k)$ is bounded since $\widehat{\boldsymbol{\phi}}(0)$ and $\boldsymbol{\phi}(k)$ are bounded. Then, the boundedness of $\widehat{\boldsymbol{\phi}}(k)$ can be derived directly.

(ii) The finite-time convergence. Let $\boldsymbol{z}(k) = [\Delta e(k)\ e(k)\ \Delta^2 e(k)]^{\mathrm{T}}$. Define a Lyapunov function

$$\mathrm{V}(k) = q_P^{-1}(k)|\Delta e(k)|^2 + q_I^{-1}(k)|e(k)|^2 + q_D^{-1}(k)|\Delta^2 e(k)|^2 = \boldsymbol{z}^{\mathrm{T}}(k)\boldsymbol{Q}^{-1}(k)\boldsymbol{z}(k). \tag{13}$$

By using the definition of $e(k)$ and LDM (5), one obtains

$$\begin{aligned}
\Delta e(k+1) &= [y^* - y(k+1)] - [y^* - y(k)] = -\Delta y(k+1) \\
&= -\phi_1(k)\Delta y(k) - \phi_2(k)\Delta y(k-1) - \phi_3(k)\Delta u(k) \\
&= \phi_1(k)\Delta e(k) + \phi_2(k)\Delta e(k-1) - \phi_3(k)\Delta u(k) \\
&= \phi_1(k)\Delta e(k) + \phi_2(k)[\Delta e(k) - \Delta^2 e(k)] - \phi_3(k)\Delta u(k) \\
&= [\phi_1(k) + \phi_2(k)]\Delta e(k) - \phi_2(k)\Delta^2 e(k) - \phi_3(k)\Delta u(k).
\end{aligned}$$

Then, by the control law (7), we have

$$\begin{aligned}
\Delta e(k+1) &= [\phi_1(k) + \phi_2(k) - \phi_3(k)\Gamma_P(k)]\Delta e(k) - \phi_3(k)\Gamma_I(k)e(k) - [\phi_2(k) + \phi_3(k)\Gamma_D(k)]\Delta^2 e(k) \\
&= [\widehat{\phi}_1(k) + \widehat{\phi}_2(k) - \widehat{\phi}_3(k)\Gamma_P(k)]\Delta e(k) - \widehat{\phi}_3(k)\Gamma_I(k)e(k) - [\widehat{\phi}_2(k) + \widehat{\phi}_3(k)\Gamma_D(k)]\Delta^2 e(k) \\
&\quad + [\widetilde{\phi}_1(k) + \widetilde{\phi}_2(k) - \widetilde{\phi}_3(k)\Gamma_P(k)]\Delta e(k) - \widetilde{\phi}_3(k)\Gamma_I(k)e(k) - [\widetilde{\phi}_2(k) + \widetilde{\phi}_3(k)\Gamma_D(k)]\Delta^2 e(k).
\end{aligned} \tag{14}$$

From (14), one has

$$\begin{aligned}
e(k+1) &= \Delta e(k+1) + e(k) \\
&= [\widehat{\phi}_1(k) + \widehat{\phi}_2(k) - \widehat{\phi}_3(k)\Gamma_P(k)]\Delta e(k) + [1 - \widehat{\phi}_3(k)\Gamma_I(k)]e(k) - [\widehat{\phi}_2(k) + \widehat{\phi}_3(k)\Gamma_D(k)]\Delta^2 e(k)
\end{aligned}$$

$$+ [\widetilde{\phi}_1(k) + \widetilde{\phi}_2(k) - \widetilde{\phi}_3(k)\Gamma_P(k)]\Delta e(k) - \widetilde{\phi}_3(k)\Gamma_I(k)e(k) - [\widetilde{\phi}_2(k) + \widetilde{\phi}_3(k)\Gamma_D(k)]\Delta^2 e(k), \quad (15)$$

and

$$\begin{aligned}\Delta^2 e(k+1) &= \Delta e(k+1) - \Delta e(k)\\ &= [\widehat{\phi}_1(k) + \widehat{\phi}_2(k) - 1 - \widehat{\phi}_3(k)\Gamma_P(k)]\Delta e(k) - \widehat{\phi}_3(k)\Gamma_I(k)e(k) - [\widehat{\phi}_2(k) + \widehat{\phi}_3(k)\Gamma_D(k)]\Delta^2 e(k)\\ &\quad + [\widetilde{\phi}_1(k) + \widetilde{\phi}_2(k) - \widetilde{\phi}_3(k)\Gamma_P(k)]\Delta e(k) - \widetilde{\phi}_3(k)\Gamma_I(k)e(k) - [\widetilde{\phi}_2(k) + \widetilde{\phi}_3(k)\Gamma_D(k)]\Delta^2 e(k).\end{aligned} \quad (16)$$

Let

$$\boldsymbol{A}(k) = \begin{bmatrix} \widehat{\phi}_1(k) + \widehat{\phi}_2(k) - \widehat{\phi}_3(k)\Gamma_P(k) & -\widehat{\phi}_3(k)\Gamma_I(k) & -\widehat{\phi}_2(k) - \widehat{\phi}_3(k)\Gamma_D(k)\\ \widehat{\phi}_1(k) + \widehat{\phi}_2(k) - \widehat{\phi}_3(k)\Gamma_P(k) & 1 - \widehat{\phi}_3(k)\Gamma_I(k) & -\widehat{\phi}_2(k) - \widehat{\phi}_3(k)\Gamma_D(k)\\ \widehat{\phi}_1(k) + \widehat{\phi}_2(k) - 1 - \widehat{\phi}_3(k)\Gamma_P(k) & -\widehat{\phi}_3(k)\Gamma_I(k) & -\widehat{\phi}_2(k) - \widehat{\phi}_3(k)\Gamma_D(k) \end{bmatrix},$$

$$\boldsymbol{B}(k) = \begin{bmatrix} \widetilde{\phi}_1(k) + \widetilde{\phi}_2(k) - \widetilde{\phi}_3(k)\Gamma_P(k) & -\widetilde{\phi}_3(k)\Gamma_I(k) & -\widetilde{\phi}_2(k) - \widetilde{\phi}_3(k)\Gamma_D(k)\\ \widetilde{\phi}_1(k) + \widetilde{\phi}_2(k) - \widetilde{\phi}_3(k)\Gamma_P(k) & -\widetilde{\phi}_3(k)\Gamma_I(k) & -\widetilde{\phi}_2(k) - \widetilde{\phi}_3(k)\Gamma_D(k)\\ \widetilde{\phi}_1(k) + \widetilde{\phi}_2(k) - \widetilde{\phi}_3(k)\Gamma_P(k) & -\widetilde{\phi}_3(k)\Gamma_I(k) & -\widetilde{\phi}_2(k) - \widetilde{\phi}_3(k)\Gamma_D(k) \end{bmatrix}.$$

Then, Eqs. (14)–(16) can be rewritten as

$$\boldsymbol{z}(k+1) = [\boldsymbol{A}(k) + \boldsymbol{B}(k)]\boldsymbol{z}(k). \quad (17)$$

By virtue of Young's inequality, it follows from (13) and (17) that $\forall \rho > 0$, one has

$$\begin{aligned}\mathrm{V}(k+1) &= \boldsymbol{z}^{\mathrm{T}}(k+1)\boldsymbol{Q}^{-1}(k+1)\boldsymbol{z}(k+1)\\ &= \boldsymbol{z}^{\mathrm{T}}(k)[\boldsymbol{A}(k) + \boldsymbol{B}(k)]^{\mathrm{T}}\boldsymbol{Q}^{-1}(k+1)[\boldsymbol{A}(k) + \boldsymbol{B}(k)]\boldsymbol{z}(k)\\ &\leqslant \left(1 + \frac{1}{\rho}\right)\boldsymbol{z}^{\mathrm{T}}(k)\boldsymbol{A}^{\mathrm{T}}(k)\boldsymbol{Q}^{-1}(k+1)\boldsymbol{A}(k)\boldsymbol{z}(k) + (1+\rho)\boldsymbol{z}^{\mathrm{T}}(k)\boldsymbol{B}^{\mathrm{T}}(k)\boldsymbol{Q}^{-1}(k+1)\boldsymbol{B}(k)\boldsymbol{z}(k).\end{aligned} \quad (18)$$

Setting

$$\boldsymbol{\Theta}(k) = \begin{bmatrix} \widetilde{\phi}_1(k) + \widetilde{\phi}_2(k) & -\widetilde{\phi}_2(k) & -\widetilde{\phi}_3(k)\\ \widetilde{\phi}_1(k) + \widetilde{\phi}_2(k) & -\widetilde{\phi}_2(k) & -\widetilde{\phi}_3(k)\\ \widetilde{\phi}_1(k) + \widetilde{\phi}_2(k) & -\widetilde{\phi}_2(k) & -\widetilde{\phi}_3(k) \end{bmatrix}, \quad \boldsymbol{B}_1(k) = \begin{bmatrix} 1 & 0 & 0\\ 0 & 0 & 1\\ \Gamma_P(k) & \Gamma_I(k) & \Gamma_D(k) \end{bmatrix},$$

we have

$$\boldsymbol{B}(k) = \boldsymbol{\Theta}(k)\boldsymbol{B}_1(k).$$

Since $\widetilde{\boldsymbol{\phi}}(k)$ is bounded, the norm of matrix $\boldsymbol{\Theta}(k)$ is also bounded. Then, for a constant $\lambda_{\min} := \|\boldsymbol{\Theta}(k)\|_{\boldsymbol{Q}^{-1}(k+1)}$, $\forall \lambda > \lambda_{\min}$, one obtains

$$\begin{aligned}\boldsymbol{z}^{\mathrm{T}}(k)\boldsymbol{B}^{\mathrm{T}}(k)\boldsymbol{Q}^{-1}(k+1)\boldsymbol{B}(k)\boldsymbol{z}(k) &= \|\boldsymbol{\Theta}(k)\boldsymbol{B}_1(k)\boldsymbol{z}(k)\|^2_{\boldsymbol{Q}^{-1}(k+1)}\\ &< \lambda^2\boldsymbol{z}^{\mathrm{T}}(k)\boldsymbol{B}_1^{\mathrm{T}}(k)\boldsymbol{Q}^{-1}(k+1)\boldsymbol{B}_1(k)\boldsymbol{z}(k).\end{aligned} \quad (19)$$

Therefore, in light of (13), (18) and (19), one has

$$\begin{aligned}&\mathrm{V}(k+1) - \mathrm{V}(k)\\ &< \left(1 + \frac{1}{\rho}\right)\boldsymbol{z}^{\mathrm{T}}(k)\boldsymbol{A}^{\mathrm{T}}(k)\boldsymbol{Q}^{-1}(k+1)\boldsymbol{A}(k)\boldsymbol{z}(k) + (1+\rho)\lambda^2\boldsymbol{z}^{\mathrm{T}}(k)\boldsymbol{B}_1^{\mathrm{T}}(k)\boldsymbol{Q}^{-1}(k+1)\boldsymbol{B}_1(k)\boldsymbol{z}(k)\\ &\quad - \boldsymbol{z}^{\mathrm{T}}(k)\boldsymbol{Q}^{-1}(k)\boldsymbol{z}(k)\end{aligned}$$

$$= \boldsymbol{z}^{\mathrm{T}}(k)\left[\boldsymbol{A}^{\mathrm{T}}(k)\left(\frac{\rho}{1+\rho}\boldsymbol{Q}(k+1)\right)^{-1}\boldsymbol{A}(k)+\boldsymbol{B}_1^{\mathrm{T}}(k)\left(\frac{1}{(1+\rho)\lambda^2}\boldsymbol{Q}(k+1)\right)^{-1}\boldsymbol{B}_1(k)-\boldsymbol{Q}^{-1}(k)\right]\boldsymbol{z}(k). \tag{20}$$

Note that by (8) one can obtain

$$\begin{aligned}\boldsymbol{A}(k)&=\boldsymbol{\Phi}_{1,2}(k)-\boldsymbol{\Phi}_3(k)\left[\Gamma_P(k)\ \Gamma_I(k)\ \Gamma_D(k)\right],\\ \boldsymbol{B}_1(k)&=\boldsymbol{C}_1+\boldsymbol{C}_2\left[\Gamma_P(k)\ \Gamma_I(k)\ \Gamma_D(k)\right],\end{aligned}$$

and

$$\begin{aligned}\boldsymbol{A}(k)\boldsymbol{Q}(k)&=\boldsymbol{\Phi}_{1,2}(k)\boldsymbol{Q}(k)-\boldsymbol{\Phi}_3(k)\boldsymbol{L}(k),\\ \boldsymbol{B}_1(k)\boldsymbol{Q}(k)&=\boldsymbol{C}_1\boldsymbol{Q}(k)+\boldsymbol{C}_2\boldsymbol{L}(k).\end{aligned}$$

Then, condition (9a) implies

$$\begin{bmatrix}-\boldsymbol{Q}(k) & * & * \\ \boldsymbol{A}(k)\boldsymbol{Q}(k) & -\frac{\rho}{1+\rho}\boldsymbol{Q}(k+1) & * \\ \boldsymbol{B}_1(k)\boldsymbol{Q}(k) & \mathbf{0} & -\frac{1}{(1+\rho)\lambda^2}\boldsymbol{Q}(k+1)\end{bmatrix}<0. \tag{21}$$

By using the arguments of Schur complements, inequality (21) can be rewritten as

$$\boldsymbol{Q}(k)\boldsymbol{A}^{\mathrm{T}}(k)\left[\frac{\rho}{1+\rho}\boldsymbol{Q}(k+1)\right]^{-1}\boldsymbol{A}(k)\boldsymbol{Q}(k)+\boldsymbol{Q}(k)\boldsymbol{B}_1^{\mathrm{T}}(k)\left[\frac{1}{(1+\rho)\lambda^2}\boldsymbol{Q}(k+1)\right]^{-1}\boldsymbol{B}_1(k)\boldsymbol{Q}(k)-\boldsymbol{Q}(k)<0. \tag{22}$$

Pre- and post-multiplying (22) by $\boldsymbol{Q}^{-1}(k)$, one obtains

$$\boldsymbol{A}^{\mathrm{T}}(k)\left[\frac{\rho}{1+\rho}\boldsymbol{Q}(k+1)\right]^{-1}\boldsymbol{A}(k)+\boldsymbol{B}_1^{\mathrm{T}}(k)\left[\frac{1}{(1+\rho)\lambda^2}\boldsymbol{Q}(k+1)\right]^{-1}\boldsymbol{B}_1(k)-\boldsymbol{Q}^{-1}(k)<0. \tag{23}$$

Thus, by virtue of (20) and (23), one gets

$$\mathrm{V}(k+1)<\mathrm{V}(k). \tag{24}$$

Combining (13), (18), and (24), one has

$$\boldsymbol{z}^{\mathrm{T}}(k+1)\boldsymbol{Q}^{-1}(k+1)\boldsymbol{z}(k+1)<\boldsymbol{z}^{\mathrm{T}}(k)\boldsymbol{Q}^{-1}(k)\boldsymbol{z}(k). \tag{25}$$

Therefore, according to (25), as well as the conditions of (2) and (9c)–(9d), one has

$$\begin{aligned}\beta(k+1)|e(k+1)|^2&<q_I^{-1}(k+1)|e(k+1)|^2\\ &\leqslant q_P^{-1}(k+1)|\Delta e(k+1)|^2+q_I^{-1}(k+1)|e(k+1)|^2+q_D^{-1}(k+1)|\Delta^2 e(k+1)|^2\\ &<q_P^{-1}(0)|\Delta e(0)|^2+q_I^{-1}(0)|e(0)|^2+q_D^{-1}(0)|\Delta^2 e(0)|^2\\ &<r(|\Delta e(0)|^2+|e(0)|^2+|\Delta^2 e(0)|^2)\leqslant c,\end{aligned}$$

$\forall k\in\{0,1,\ldots,K-1\}$, which implies

$$\beta(K)|e(K)|^2<c.$$

Further, by selecting $\beta(k):=\theta^{K-k}$ with $0<\theta<1$, we obtain

$$|e(K)|^2<c.$$

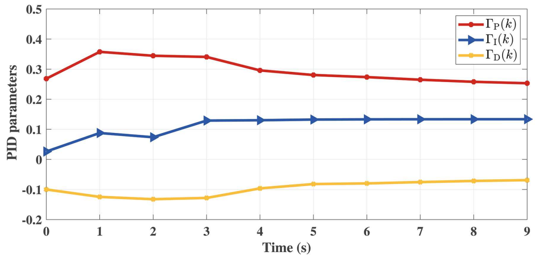

Figure 1 (Color online) Controller parameters with $c = 0.1$.

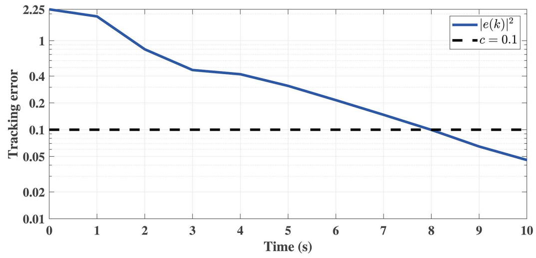

Figure 2 (Color online) Square of the tracking error with $c = 0.1$.

Corollary 1. For nonlinear discrete-time system (1) under Assumptions 1 and 2 with $y_d(k) = y^* =$ const., the PID controller (6)–(8) with the tuning law (9a)–(9b) can achieve an asymptotic convergence when the time approaches infinity, i.e., $\lim_{k\to\infty} |e(k)| = 0$.

Proof. By virtue of (20)–(25), the tuning law (9a)–(9b) can guarantee that a time-varying parameter $0 < \alpha(k) < 1$ always exists to satisfy

$$\boldsymbol{z}^{\mathrm{T}}(k+1)\boldsymbol{Q}^{-1}(k+1)\boldsymbol{z}(k+1) \leqslant \alpha(k)\boldsymbol{z}^{\mathrm{T}}(k)\boldsymbol{Q}^{-1}(k)\boldsymbol{z}(k) \leqslant \cdots \leqslant \prod_{i=0}^{k}\alpha(i)\boldsymbol{z}^{\mathrm{T}}(0)\boldsymbol{Q}^{-1}(0)\boldsymbol{z}(0). \tag{26}$$

As a result, we have $\lim_{k\to\infty} \boldsymbol{z}^{\mathrm{T}}(k)\boldsymbol{Q}^{-1}(k)\boldsymbol{z}(k) = 0$. Then by the equivalence of the norms of $\|\boldsymbol{z}(k)\|_{\boldsymbol{Q}^{-1}(k)}$ and $\|\boldsymbol{z}(k)\|$, we have $\lim_{k\to\infty} \|\boldsymbol{z}(k)\| = 0$ and $\lim_{k\to\infty} |e(k)| = 0$, since $\lim_{k\to\infty} \prod_{i=0}^{k} \alpha(i) = 0$. So, the tracking error achieves an asymptotic convergence.

Remark 5. It is noteworthy that, by virtue of both Theorem 1 and Corollary 1, the parameter updating algorithms (8) and (9) can be regarded as a tuning method of the PID controller similar to the ones in [15–19]. For the predesignated time instant K, it can be considered that the parameters have been tuned appropriately if the tracking error satisfies the error precision c. Then, one can directly fix the tuned controller parameters for the later control operations.

5 Simulation results

Consider a nonlinear system,

$$y(k+1) = \frac{y(k)}{1+y(k)^2} + u(k)^3 + w(k+1),\ k \in \mathbb{N}_+, \tag{27}$$

where $w(k)$ is an exogenous disturbance randomly varying in $[-0.01, 0.01]$.

The target trajectory is $y_d(k) = 1.5$.

Note that the system model (27) is not used for the controller design and implementation, but only generates I/O data in the simulation experiment.

The error bound is specified as $c = 0.1$ and the finite-time instant is predesignated as $K = 10$, i.e., $|e(10)|^2 < 0.1$.

Set $r = 0.014$, $\theta = 0.25$, $\eta = 1$, $\mu = 0.9$, $\lambda = 0.1$, $\rho = 1.5$; select $y(0) = 0$, $u(0) = 0.5$, and $\widehat{\boldsymbol{\phi}}(0) = [2\ 1\ 10]^{\mathrm{T}}$. It is clear that the parameter $r < \frac{c}{|e(0)|^2+|\Delta e(0)|^2+|\Delta^2 e(0)|^2} = 0.0148$ satisfies the condition (i) in Definition 1.

Then, applying the proposed FT-PID control (6)–(9), the results are shown in Figures 1–3.

From Figure 1, one can see that the three controller parameters vary with time such that the finite-time convergence can be achieved as shown in Figure 2, i.e., $|e(10)|^2 < 0.1$.

Figure 3 shows the input profile within the first 10 time instants, from which one can see that the input signal is bounded with no abrupt change, which is implementable for a practical actuator.

To verify that one can achieve other different error bounds within the same finite time instant, $K = 10$, we set $c = 0.05$. That is, our purpose is to achieve that $|e(10)|^2 < 0.05$.

Set $r = 0.007$, $\theta = 0.25$, $\eta = 1$, $\mu = 0.4$, $\lambda = 0.1$, $\rho = 1.5$, $y(0) = 0$, $u(0) = 0.5$, and $\widehat{\boldsymbol{\phi}}(0) = [2\ 1\ 10]^{\mathrm{T}}$. It is clear that $r < \frac{c}{|e(0)|^2+|\Delta e(0)|^2+|\Delta^2 e(0)|^2} = 0.0074$ also satisfies the condition (i) in Definition 1. By applying the proposed FT-PID control (6)–(9), the results are shown in Figures 4 and 5.

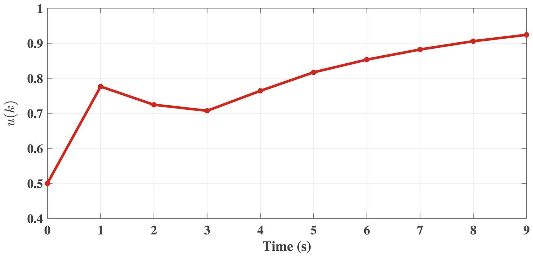

Figure 3 (Color online) Control input with $c = 0.1$.

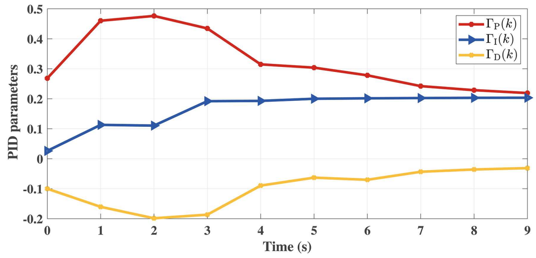

Figure 4 (Color online) Controller parameters with $c = 0.05$.

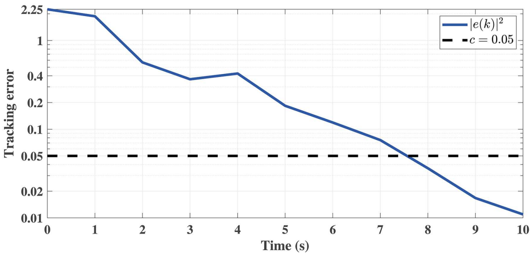

Figure 5 (Color online) Square of the tracking error with $c = 0.05$.

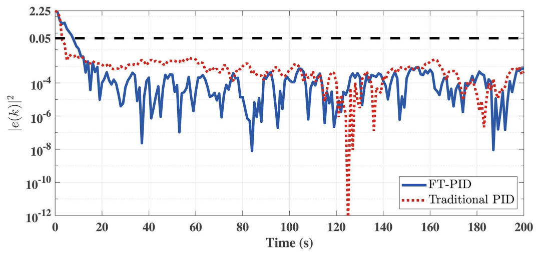

Figure 6 (Color online) Comparison of asymptotic convergence using FT-PID and traditional PID.

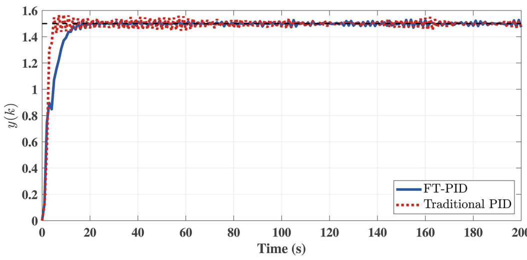

Figure 7 (Color online) Comparison of system output using FT-PID and traditional PID.

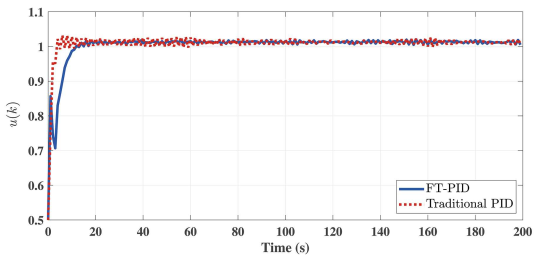

Figure 8 (Color online) Comparison of control input using FT-PID and traditional PID.

Furthermore, to verify the conclusion stated in Remark 5, when $k \geqslant 10$ we set the parameters of the control law (7) to be the values obtained at the 9-th time instant, i.e., $\Gamma_P(9)$, $\Gamma_I(9)$, $\Gamma_D(9)$, which are not further updated with the increasing time instant.

The prescribed error bound and finite-time instant are $c = 0.05$ and $K = 10$, respectively. So, under the same simulation settings as that in the previous case of $c = 0.05$, applying the proposed FT-PID control method (6)–(9) from $t = 0$ to 9, and only applying the PID control law (7) by setting the control parameters as the values obtained at the 10th time instant, i,e., $\Gamma_P(9)$, $\Gamma_I(9)$, $\Gamma_D(9)$, after the specified $K = 10$ time instant, the results are shown in Figures 6–8.

From Figures 6 and 7, one can see that the tracking error does not exceed the specified bound after the 10th time instant and achieves an asymptotic convergence with the increasing time instant although the controller parameters remain unchanged when $k \geqslant 10$. From Figure 8, one can see that the corresponding control input trajectory does not vary abruptly for all time instants although the specified error precision is required to be achieved within the predesignated finite-time. Besides, from the profile of the first 10 time instants in Figure 8, it is also illustrated that the control input is still bounded and remains smooth although it is required to achieve a prespecified error precision ($c = 0.05$) within the predesignated time instant ($K = 10$).

For a comparison, we also adopt a traditional PID controller [49],

$$u(k) = u(k-1) + \overline{\Gamma}_P \Delta e(k) + \overline{\Gamma}_I e(k) + \overline{\Gamma}_D \Delta^2 e(k), \tag{28}$$

where $\overline{\Gamma}_P$, $\overline{\Gamma}_I$ and $\overline{\Gamma}_D$ are the constant parameters.

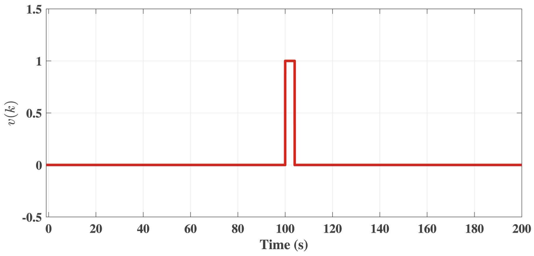

Figure 9 (Color online) Additional step disturbance at the 100th time instant.

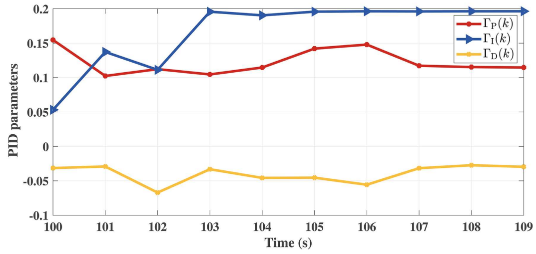

Figure 10 (Color online) Controller parameters in 100–109 time instants.

The only difference between it and the proposed FT-PID control (6)–(9) is that the parameters of the traditional PID control are not updated in real time but remain unchanged once selected properly.

With the same initial value setting, choosing $\overline{\Gamma}_P = 0.05$, $\overline{\Gamma}_I = 0.25$, and $\overline{\Gamma}_D = 0.05$, then applying the PID controller (28), the results are shown in Figures 6 and 7. It is clear that the traditional PID controller (28) can also perform well for a regulation problem. However, the proposed FT-PID control method (6)–(9) performs better than the traditional PID controller (28) not only with smaller output errors (Figure 6) but also with less overshoot, shorter regulation time, and smaller oscillation (Figure 7).

To further compare the control performance quantitatively, we define a performance index of integrated time and absolute error (ITAE), i.e., $\sum_{k=0}^{200} k|e(k)|$. One can obtain that the ITAE by applying the proposed FT-PID control is 238.38 and the one by applying the traditional PID control is 418.37. Therefore, we can again conclude that the proposed FT-PID control (6)–(9) outperforms the traditional PID controller (28) for a regulation problem with an infinite time interval.

Now, let us show the effect of a large disturbance at some operation point on the performance of the proposed FT-PID control. So, the system becomes

$$y(k+1) = \frac{y(k)}{1+y(k)^2} + u(k)^3 + w(k+1) + v(k+1), \tag{29}$$

where $v(k)$ is an additional step disturbance at the 100th time instant as shown in Figure 9.

The specified error bound is $c = 0.05$. Due to the large disturbance $v(k)$ suddenly added to the system, it is clear the regulation error exceeds the specified error region. So, we can again tune the controller parameters $\Gamma_P(k)$, $\Gamma_I(k)$, and $\Gamma_D(k)$ according to (8) and (9) by setting $k \in \{100, \ldots, 100+K\}$ and $K = 10$.

When recomputing the controller parameters by applying the FT-PID control (6)–(9), setting $r = 0.016 < \frac{c}{|e(100)|^2+|\Delta e(100)|^2+|\Delta^2 e(100)|^2} = 0.0165$, and choosing θ, η, μ, λ, and ρ the same as the previous case of $c = 0.05$, the initial value $\widehat{\boldsymbol{\phi}}(100)$ is set the same as $\widehat{\boldsymbol{\phi}}(9)$. Then, applying the proposed FT-PID control (6)–(9) again, the results are shown in Figures 10 and 11.

From Figure 10, one can see the recomputed three controller parameters vary with time instants too. The finite-time convergence can be achieved as shown in Figure 11, i.e., $|e(100+K)|^2 < 0.05$. In addition, when $k \geqslant 100+K$ we set the parameters of the control law (7) to $\Gamma_P(109)$, $\Gamma_I(109)$, $\Gamma_D(109)$, and they will be not further updated with the increasing time instant. One can see from Figure 11 that an asymptotic convergence is achieved.

For comparison, we apply the control law (7) with parameters $\Gamma_P(9)$, $\Gamma_I(9)$, $\Gamma_D(9)$ tuned by the FT-PID control (6)–(9) in the first 10 time instants and the traditional PID controller (28) with the same controller parameters as the previous example, one can see from Figure 11 that both the two PID controllers can also guarantee their asymptotic convergence. However, the FT-PID control with recomputed parameters can make the tracking error converge inside $c = 0.05$ more quickly and thus it performs better than the FT-PID control with the parameters obtained at the end of the finite-time interval. Further, the FT-PID with recomputed parameters also achieves a performance superior to that of the traditional PID control as shown in Figure 11.

To further compare the control performance quantitatively, we compute the ITAE $= \sum_{k=0}^{200} k|e(k)|$ of the tracking error after applying the three PID controllers. The ITAE by applying the FT-PID controller with parameters tuned by the FT-PID control in the first 10 time instants is 634.71, the one by applying the traditional PID is 721.67, and the one by applying the FT-PID controller with recomputed

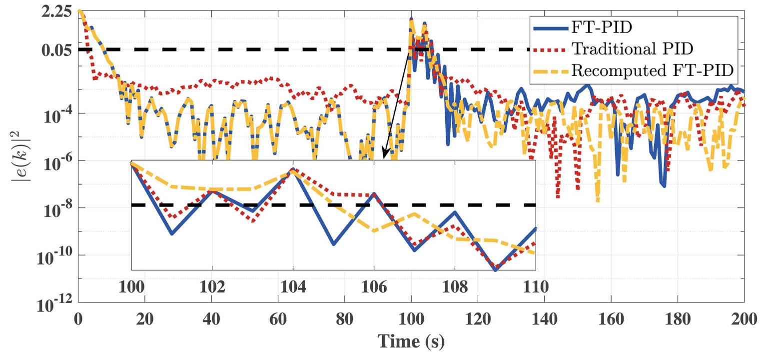

Figure 11 (Color online) Asymptotic convergence under impulsive disturbance.

parameters is 539.06. Therefore, we can again conclude that the FT-PID control with recomputed parameters outperforms the other two controllers.

6 Conclusion

A novel FT-PID control is proposed for nonaffined nonlinear systems under the data-driven framework. The proposed scheme includes an incremental PID control law, an adaptive tuning algorithm for the three PID parameters, a set of LMIs, and a pseudo gradient vector estimation algorithm. By virtue of the three time-varying parameters obtained by solving the LMIs, one can guarantee the error of the FT-PID converges to a predesignated precision within the finite-time instant that is predesignated beforehand. The proposed FT-PID control is data-driven and thus is capable of dealing with complex nonlinear systems. The convergence analysis is conducted by a new Lyapunov function and the Young's inequality. The simulation study further verifies the results.

Acknowledgements This work was supported partially by National Natural Science Foundation of China (Grant Nos. 62203245, 62273192, 62003097) and Talent Introduction and Cultivation Plan for Youth Innovation of Universities in Shandong Province, China.

References

1 Minorsky N. Directional stability of automatically steered bodies. J Am Soc Naval Eng, 1922, 34: 280–309
2 Norambuena M, Rodriguez J, Zhang Z, et al. A very simple strategy for high-quality performance of AC machines using model predictive control. IEEE Trans Power Electron, 2018, 34: 794–800
3 Yin Y, Liu J, Marquez A, et al. Advanced control strategies for DC-DC buck converters with parametric uncertainties via experimental evaluation. IEEE Trans Circ Syst I, 2020, 67: 5257–5267
4 Miranda-Colorado R, Aguilar L T. Robust PID control of quadrotors with power reduction analysis. ISA Trans, 2020, 98: 47–62
5 Ghith E S, Tolba F A A. Design and optimization of PID controller using various algorithms for micro-robotics system. J Robot Control, 2022, 3: 244–256
6 Zhao C, Guo L. PID controller design for second order nonlinear uncertain systems. Sci China Inf Sci, 2017, 60: 022201
7 Zhang J, Guo L. Theory and design of PID controller for nonlinear uncertain systems. IEEE Control Syst Lett, 2019, 3: 643–648
8 Guo L. Estimation, control, and games of dynamical systems with uncertainty (in Chinese). Sci Sin Inform, 2020, 50: 1327–1344
9 Åström K J, Hägglund T. PID Controllers: Theory, Design, and Tuning. Research Triangle Park: Instrument Society of America, 1995
10 Kumar V, Patra A. Application of Ziegler-Nichols method for tuning of PID controller. In: Proceedings of the 2nd International Conference on Recent Innovations in Science, Technology, Management and Environment, New Delhi, 2016. 559–570
11 Chidambaram M, Saxena N. Relay Tuning of PID Controllers. Tamil Nadu: Springer, 2018
12 Joseph E A, Olaiya O O. Cohen-coon PID tuning method: a better option to Ziegler Nichols-PID tuning method. Comput Eng Intell Syst, 2018, 9: 33–37
13 Campi M C, Savaresi S M. Direct nonlinear control design: the virtual reference feedback tuning (VRFT) approach. IEEE Trans Automat Contr, 2006, 51: 14–27
14 Son D, Choi H. Iterative feedback tuning of the proportional-integral-differential control of flow over a circular cylinder. IEEE Trans Contr Syst Technol, 2018, 27: 1385–1396
15 Huang H P, Jeng J C, Roan M L. On-line adaptive tuning for PID controllers. IEE Proc-Control Theor Appl, 2002, 149: 60–67
16 Borase R P, Maghade D K, Sondkar S Y, et al. A review of PID control, tuning methods and applications. Int J Dynam Control, 2021, 9: 818–827
17 Singhal K, Kumar V, Rana K P S. Robust trajectory tracking control of non-holonomic wheeled mobile robots using an adaptive fractional order parallel fuzzy PID controller. J Franklin Inst, 2022, 359: 4160–4215

18 Jabeur C B, Seddik H. Optimized neural networks-PID controller with wind rejection strategy for a quad-rotor. J Robot Control, 2022, 3: 62–72
19 Juang J G, Huang M T, Liu W K. PID control using presearched genetic algorithms for a MIMO system. IEEE Trans Syst Man Cybern C, 2008, 38: 716–727
20 Wang N, Gao Y, Yang C, et al. Reinforcement learning-based finite-time tracking control of an unknown unmanned surface vehicle with input constraints. Neurocomputing, 2022, 484: 26–37
21 Du H, Li S, Qian C. Finite-time attitude tracking control of spacecraft with application to attitude synchronization. IEEE Trans Automat Contr, 2011, 56: 2711–2717
22 Hong Y, Xu Y, Huang J. Finite-time control for robot manipulators. Syst Control Lett, 2002, 46: 243–253
23 Dorato P. Short Time Stability in Linear Time-varying Systems. Research Report No. PIBMRI-908-61, 1961
24 Rang E. Isochrone families for second-order systems. IEEE Trans Automat Contr, 1963, 8: 64–65
25 Weiss L, Infante E. Finite time stability under perturbing forces and on product spaces. IEEE Trans Automat Contr, 1967, 12: 54–59
26 Xiong X L, Yang X S, Cao J D, et al. Finite-time control for a class of hybrid systems via quantized intermittent control. Sci China Inf Sci, 2020, 63: 192201
27 Amato F, Ariola M. Finite-time control of discrete-time linear systems. IEEE Trans Automat Contr, 2005, 50: 724–729
28 He X Y, Wang Q Y, Hao Y Q. Finite-time adaptive formation control for multi-agent systems with uncertainties under collision avoidance and connectivity maintenance. Sci China Tech Sci, 2020, 63: 2305–2314
29 Amato F, Ariola M, Cosentino C. Finite-time stability of linear time-varying systems: analysis and controller design. IEEE Trans Automat Contr, 2010, 55: 1003–1008
30 Amato F, Ambrosino R, Ariola M, et al. Input to output finite-time stabilization of discrete-time linear systems. In: Proceedings of the 18th World Congress The International Federation of Automatic Control Milano, 2011. 156–161
31 Huang S, Xiang Z, Karimi H R. Input-output finite-time stability of discrete-time impulsive switched linear systems with state delays. Circ Syst Signal Process, 2014, 33: 141–158
32 Zhao Y, Liu Y, Ma Y. Robust finite-time sliding mode control for discrete-time singular system with time-varying delays. J Franklin Inst, 2021, 358: 4848–4863
33 Li Y, Qu F, Tong S. Observer-based fuzzy adaptive finite-time containment control of nonlinear multiagent systems with input delay. IEEE Trans Cybern, 2021, 51: 126–137
34 Li Y, Fan Y, Li K, et al. Adaptive optimized backstepping control-based RL algorithm for stochastic nonlinear systems with state constraints and its application. IEEE Trans Cybern, 2022, 52: 10542–10555
35 Haddad W M, Lee J. Finite-time stability of discrete autonomous systems. Automatica, 2020, 122: 109282
36 Haddad W M, Lee J. Finite-time stabilization and optimal feedback control for nonlinear discrete-time systems. IEEE Trans Automat Contr, 2022, 68: 1685–1691
37 Lee J, Haddad W M, Lanchares M. Finite time stability and optimal finite time stabilization for discrete-time stochastic dynamical systems. IEEE Trans Automat Contr, 2023, 68: 3978–3991
38 Min H, Xu S, Gu J, et al. Adaptive finite-time stabilization of nonlinearly parameterized systems subject to mismatching disturbances. Intl J Robust Nonlinear, 2019, 29: 3469–3484
39 Yao D, Liu X, Wu J. Adaptive finite-time tracking control for class of uncertain nonlinearly parameterized systems with input delay. Int J Control Autom Syst, 2020, 18: 2251–2258
40 Li Y, Li K, Tong S. Adaptive neural network finite-time control for multi-input and multi-output nonlinear systems with positive powers of odd rational numbers. IEEE Trans Neural Netw Learn Syst, 2020, 31: 2532–2543
41 Li Y, Yang T, Tong S. Adaptive neural networks finite-time optimal control for a class of nonlinear systems. IEEE Trans Neural Netw Learn Syst, 2020, 31: 4451–4460
42 Wang H, Chen M, Liu X. Fuzzy adaptive fixed-time quantized feedback control for a class of nonlinear systems. Acta Autom Sin, 2021, 47: 2823–2830
43 Wang H, Xu K, Zhang H. Adaptive finite-time tracking control of nonlinear systems with dynamics uncertainties. IEEE Trans Automat Contr, 2023, 68: 5737–5744
44 Hou Z, Jin S. Model Free Adaptive Control: Theory and Applications. New York: CRC Press, 2013
45 Hou Z, Xiong S. On model-free adaptive control and its stability analysis. IEEE Trans Automat Contr, 2019, 64: 4555–4569
46 Moharana R. Review on Young's inequality. Dissertation for Ph.D. Degree. Rourkela: National Institute Of Technology Rourkela, 2014
47 Johansson R. Adaptive control of robot manipulator motion. IEEE Trans Robot Autom, 1990, 6: 483–490
48 Manring N D, Fales R C. Hydraulic Control Systems. Hoboken: John Wiley and Sons, 2019
49 Xiong S, Hou Z. Stabilizing regions of PID controller for a class of unknown nonlinear non-affine discrete-time systems. Int J Robust Nonlinear, 2022, 32: 9421–9437

Appendix A Proof of Lemma 1

Proof. From nonlinear system (1), one has

$$\begin{aligned}\Delta y(k+1) =& f\left(y(k),\ y(k-1),\ldots,y(k-n_y),u(k),\ u(k-1),\ldots,u(k-n_u)\right)\\&- f\left(y(k-1),\ y(k-2),\ldots,y(k-n_y-1),u(k-1),\ u(k-2),\ldots,u(k-n_u-1)\right)\\=& f\left(y(k),\ y(k-1),\ldots,y(k-n_y),u(k),\ u(k-1),\ldots,u(k-n_u)\right)\\&- f\left(y(k-1),\ y(k-1),\ldots,y(k-n_y),u(k),\ u(k-1),\ldots,u(k-n_u)\right)\\&+ f\left(y(k-1),\ y(k-1),\ldots,y(k-n_y),u(k),\ u(k-1),\ldots,u(k-n_u)\right)\\&- f\left(y(k-1),\ y(k-1),\ldots,y(k-n_y),u(k-1),\ u(k-1),\ldots,u(k-n_u)\right)\\&+ f\left(y(k-1),\ y(k-1),\ldots,y(k-n_y),u(k-1),\ u(k-1),\ldots,u(k-n_u)\right)\\&- f\left(y(k-1),\ y(k-2),\ldots,y(k-n_y-1),u(k-1),\ u(k-2),\ldots,u(k-n_u-1)\right).\end{aligned}\qquad\text{(A1)}$$

By utilizing Assumptions 1 and 2, and Cauchy's mean value theorem, Eq. (A1) can be rewritten as

$$\Delta y(k+1) = \frac{\partial f}{\partial y(k)}\Delta y(k) + \frac{\partial f}{\partial u(k)}\Delta u(k) + f\left(y(k-1),\ y(k-1),\ldots,y(k-n_y),u(k-1),\ u(k-1),\ldots,u(k-n_u)\right)$$

$$- f\left(y(k-1),\ y(k-2),\ldots,y(k-n_y-1),u(k-1),\ u(k-2),\ldots,u(k-n_u-1)\right), \tag{A2}$$

where $\frac{\partial f}{\partial y(k)}$ is the partial derivatives of $f(\cdot)$ with respect to the 1st variable at a certain point between

$$\left[y(k),\ y(k-1),\ y(k-2),\ldots,y(k-n_y),u(k),\ u(k-1),\ u(k-2),\ldots,u(k-n_u)\right]^{\mathrm{T}}$$

and

$$\left[y(k-1),\ y(k-1),\ y(k-2),\ldots,y(k-n_y),u(k),\ u(k-1),\ u(k-2),\ldots,u(k-n_u)\right]^{\mathrm{T}},$$

and $\frac{\partial f}{\partial u(k)}$ is the the partial derivatives of $f(\cdot)$ with respect to the (n_y+2)-th variable at a certain point between

$$\left[y(k-1),\ y(k-1),\ y(k-2),\ldots,y(k-n_y),u(k),\ u(k-1),\ u(k-2),\ldots,u(k-n_u)\right]^{\mathrm{T}}$$

and

$$\left[y(k-1),\ y(k-1),\ y(k-2),\ldots,y(k-n_y),u(k-1),\ u(k-1),\ u(k-2),\ldots,u(k-n_u)\right]^{\mathrm{T}}.$$

Letting

$$\begin{aligned}
&\psi\left(y(k-1),\ y(k-2),\ldots,y(k-n_y-1),u(k-1),\ u(k-2),\ldots,u(k-n_u-1)\right)\\
&= f\left(y(k-1),\ y(k-1),\ldots,y(k-n_y),u(k-1),\ u(k-1),\ldots,u(k-n_u)\right)\\
&\quad - f\left(y(k-1),\ y(k-2),\ldots,y(k-n_y-1),u(k-1),\ u(k-2),\ldots,u(k-n_u-1)\right),
\end{aligned}$$

Eq. (A2) becomes

$$\begin{aligned}
\Delta y(k+1) &= \frac{\partial f}{\partial y(k)}\Delta y(k) + \frac{\partial f}{\partial u(k)}\Delta u(k)\\
&\quad + \psi\left(y(k-1),\ y(k-2),\ldots,y(k-n_y-1),u(k-1),\ u(k-2),\ldots,u(k-n_u-1)\right)\\
&= \frac{\partial f}{\partial y(k)}\Delta y(k) + \frac{\partial f}{\partial u(k)}\Delta u(k)\\
&\quad + \psi\left(y(k-1),\ y(k-2),\ldots,y(k-n_y-1),u(k-1),\ u(k-2),\ldots,u(k-n_u-1)\right)\\
&\quad - \psi\left(y(k-2),\ y(k-2),\ldots,y(k-n_y-1),u(k-1),\ u(k-2),\ldots,u(k-n_u-1)\right)\\
&\quad + \psi\left(y(k-2),\ y(k-2),\ldots,y(k-n_y-1),u(k-1),\ u(k-2),\ldots,u(k-n_u-1)\right)\\
&= \frac{\partial f}{\partial y(k)}\Delta y(k) + \frac{\partial f}{\partial u(k)}\Delta u(k) + \frac{\partial \psi}{\partial y(k-1)}\Delta y(k-1)\\
&\quad + \psi\left(y(k-2),\ y(k-2),\ldots,y(k-n_y-1),u(k-1),\ u(k-2),\ldots,u(k-n_u-1)\right),
\end{aligned} \tag{A3}$$

where $\frac{\partial \psi}{\partial y(k-1)}$ is the partial derivatives of $\psi(\cdot)$ with respect to the 1st variable at a certain point between

$$\left[y(k-1),\ y(k-2),\ y(k-3),\ldots,y(k-n_y-1),u(k-1),\ u(k-2),\ u(k-3),\ldots,u(k-n_u-1)\right]^{\mathrm{T}}$$

and

$$\left[y(k-2),\ y(k-2),\ y(k-3),\ldots,y(k-n_y-1),u(k-1),\ u(k-2),\ u(k-3),\ldots,u(k-n_u-1)\right]^{\mathrm{T}}.$$

Consider the following equation with a vector-valued variable $\boldsymbol{\vartheta}(k) \in \mathbb{R}^3$,

$$\begin{aligned}
&\psi\left(y(k-2),\ y(k-2),\ldots,y(k-n_y-1),u(k-1),\ u(k-2),\ldots,u(k-n_u-1)\right)\\
&= \boldsymbol{\vartheta}^{\mathrm{T}}(k)\left[\Delta y(k)\ \ \Delta y(k-1)\ \ \Delta u(k)\right]^{\mathrm{T}}\\
&= \boldsymbol{\vartheta}^{\mathrm{T}}(k)\Delta \boldsymbol{h}(k).
\end{aligned} \tag{A4}$$

Since this work aims at a bounded tracking performance, i.e., the tracking error is not necessarily zero, according to (7), we have $\|\Delta \boldsymbol{h}(k)\| \neq 0$. So, one can find a bounded matrix $\boldsymbol{\vartheta}_1(k)$ satisfying (A4).

Then, we have (5) with

$$\boldsymbol{\phi}(k) = \boldsymbol{\vartheta}_1(k) + \left[\frac{\partial f}{\partial y(k)}\ \ \frac{\partial \psi}{\partial y(k-1)}\ \ \frac{\partial f}{\partial u(k)}\right]^{\mathrm{T}},$$

which is bounded by Assumption 2.

Therefore, the conclusion of Lemma 1 is proved.